Journal of Alloys and Compounds 509 (2011) 9387–9393

Contents lists available at ScienceDirect

Journal of Alloys and Compounds

journal homepage: www.elsevier.com/locate/jallcom

Modeling the initiation of dynamic recrystallization using a dynamic recovery model

A. Momeni [a,*], K. Dehghani [a], G.R. Ebrahimi [b]

[a] Department of Mining and Metallurgical Eng., AmirKabir University of Technology, Tehran, Iran
[b] Metallurgy and Materials Engineering Department, Sabzevar Tarbiat Moallem University, Sabzevar, Iran

ARTICLE INFO

Article history:
Received 26 May 2011
Received in revised form 5 July 2011
Accepted 6 July 2011
Available online 23 July 2011

Keywords:
Hot working
Thermomechanical processing
Dislocation density
Hot compression test
Stainless steel

ABSTRACT

Dynamic recrystallization flow curve was studied in AISI 410 martensitic stainless steel by performing hot compression tests in a temperature range of 900–1150 °C and at strain rates of 0.001–1 s^{-1}. The Estrin and Mecking's equation for dynamic recovery was used to model the work hardening region of the flow curves. The critical strain and stress for the initiation of dynamic recrystallization were determined using the method developed by Poliak and Jonas. The critical dislocation density for starting dynamic recrystallization was estimated using the Estrin and Mecking's dynamic recovery model. A modified Arrhenius-type equation was used to relate the critical dislocation density to strain rate and temperature. The proposed model was also verified by the model proposed by Roberts and Ahlblom and developed to describe the variation of dislocation density and fractional softening due to dynamic recrystallization up to the peak of flow curve.

1. Introduction

Dynamic recrystallization (DRX) is the most important microstructural phenomenon during the hot deformation of austenite in stainless steels [1–6]. As DRX often results in grain refining, taking advantage of this process during hot working has been of great interest [7–12]. In alloys with low stacking fault energy (SFE), such as austenite phase, the processes of dislocations annihilation and rearrangement associated with dynamic recovery (DRV) proceeds sluggishly. This leads to the build-up of dislocation density until reaching a critical value for triggering DRX. Although DRX and DRV are known to be competitive, DRV essentially plays an important role in the initiation of DRX. In a representative flow curve of DRX, flow stress increases up to a peak where DRX actually comes into operation and leads to a pronounced flow softening. When the flow softening due to DRX balances the work hardening, flow stress attains a steady state region.

Many attempts have been devoted to model a typical flow curve of DRX. Different flow behaviors before and after the peak have obliged researchers to establish respective constitutive models for each region. The Avrami-type equations often have been used to model the flow softening due to DRX [13–16]. Otherwise, different approaches were taken to model the material flow up to the peak. In this way, different evolutionary laws describing the variation of dislocation density under the concurrent influence of DRV and work hardening have been used [17–19]. The evolution law proposed by Estrin and Mecking [20] has been widely used in the literature to model the variation of dislocation density with strain. The proposed models were firstly used to formulate the flow curves of high SFE materials characterized by DRV. However, they were also useful to describe the work hardening region of the DRX flow curve in low and medium SFE materials. On the other hand, some efforts were made to model the work hardening region of the DRX flow curve using the empirical equations. Cingara and Mcqueen [21] described the work hardening region of the flow curve of different austenitic stainless steels by an exponential equation in which peak strain and stress were used as empirical constants. Considering the fact that DRX starts actually before the peak, both aforementioned approaches are not well representing the contribution of DRV in the initiation of DRX. Hence, the present research has been devoted to develop the current understanding of the dislocation evolution approach for the formulation of DRX curve and to clarify its link with the preceding DRV.

2. Materials and methods

The material used in this investigation was AISI 410 martensitic stainless steel whose chemical composition is given in Table 1. Cylindrical compression samples of 15 mm height and 10 mm diameter were prepared from the as-received hot forged bar according to the ASTM E209. Lubrication of samples surfaces was done to minimize the effect of friction between the contacting surfaces of samples and anvils. A Zwick Roell 250 testing machine was used to perform hot compression tests. Before testing, all the specimens were reheated to 1200 °C, held for 15 min followed by cooling down to testing temperature. After soaking for 2 min at testing

* Corresponding author. Tel.: +98 9123349007.
E-mail address: ammomeni@aut.ac.ir (A. Momeni).

0925-8388/$ – see front matter © 2011 Elsevier B.V. All rights reserved.
doi:10.1016/j.jallcom.2011.07.014

Table 1
Chemical composition of AISI 410 martensitic stainless steel used in the present investigation.

Cr	Mn	Si	C	P	S	Fe
13.00	1.00	0.80	0.06	0.04	0.03	Balance

temperature, hot compression tests were carried out in a temperature range of 900–1150 °C and at strain rates of 10^{-3} to $1\,s^{-1}$ with the interval of an order of magnitude [13].

3. Results and discussion

3.1. Constitutive analysis

The flow curves and the constitutive analysis of flow stress data were detailed in the previous paper published by the authors elsewhere [13]. Using the equation of hyperbolic sine function proposed by Sellars and Tegart [22] flow stress of the studied alloy is correlated to the Zener–Hollomon parameter (Z) as follows [13]:

$$Z = \dot{\varepsilon} \exp\left(\frac{448,000}{8.314T}\right) = 2.2 \times 10^{16}[\sinh(0.011\,\sigma)]^{4.9} \quad (1)$$

The peak of a typical DRX curve is a characteristic point that plays an important role in modeling and the interpretation of flow curve. This is because the dependence of peak strain and stress to the Z parameter is of great importance. The following power-law equations can be used to define the relation between the peak position and deformation regime [13]:

$$\sigma_p = 0.27Z^{0.15} \quad (2)$$

$$\varepsilon_p = 0.003Z^{0.12} \quad (3)$$

According to the equations, with an increase in Z value, the stress and strain of peak are shifted to higher strains. That is because the higher strain rate or lower temperature slows down the process of nucleation and growth of DRX grains. Moreover, higher Z value increases the rate of dislocation generation leading to an increase in flow stress level.

3.2. Description of work hardening

The evolution of dislocation density with strain during hot working is controlled by the generation and annihilation of dislocations during work hardening and DRV, respectively. Hence, the evolution law can be assumed as the sum of differential hardening and softening terms:

$$\frac{d\rho}{d\varepsilon} = \left(\frac{d\rho}{d\varepsilon}\right)^{+} + \left(\frac{d\rho}{d\varepsilon}\right)^{-} \quad (4)$$

where ρ is the dislocation density. On the right-hand side of Eq. (4), the first term stands for work hardening part and the second term denotes the contribution of DRV. In the present study, the dependence of the dislocation density on plastic strain is expressed by the equation proposed by Estrin and Mecking [20]:

$$\frac{d\rho}{d\varepsilon} = h - r\rho \quad (5)$$

where h is the athermal work-hardening rate and r denotes the rate of dynamic recovery at a given temperature and strain rate. Both h and r are considered independent of the applied strain. The above differential equation gives rise to the following description of flow stress:

$$\sigma = [\sigma_{rec}^2 - (\sigma_{rec}^2 - \sigma_0^2)\exp(-r\varepsilon)]^{0.5} \quad (6)$$

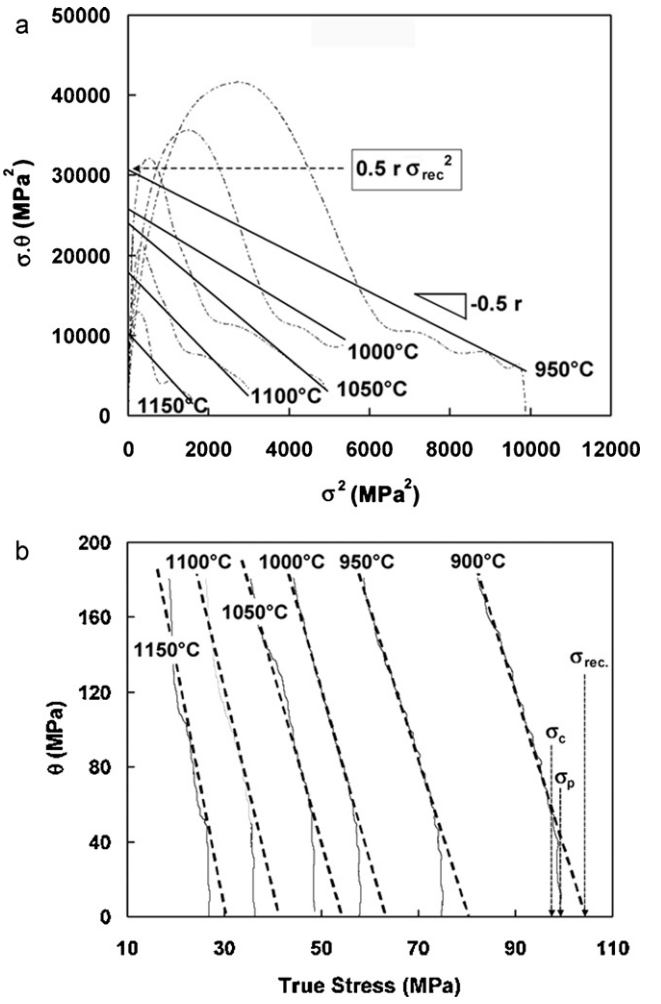

Fig. 1. (a) Plots of $\theta\sigma$ against σ^2 used for the determination of dynamic recovery factor, r, and the steady state stress, σ_{rec}, according to Eq. (14), (b) θ–σ curves where the critical stress for the initiation of DRX, σ_c, is determined by the Poliak and Jonas method.

where σ_{rec} and σ_0 denote the initial and saturated stress defined as $(\alpha MGb)^2(h/r)$ and $(\alpha MGb)^2\rho_0$, respectively. α is a shape factor in the order of unity, M is the Taylor factor (3.07 for FCC materials), G is the shear modulus, b is the magnitude of Burger's vector and ρ_0 is the initial dislocation density. Work hardening rate at the early stages of deformation is high enough to justify the simplifying assumption that ρ_0 is nearly negligible as compared to the stored dislocation density during hot deformation. This assumption is also more pertinent to a low SFE material such as austenite characterized by a sluggish DRV. Therefore, in the formulation of flow curve using Eq. (6), σ_0 can be neglected and the simplified description of work hardening curve can be as follows:

$$\sigma = \sigma_{rec}(1 - \exp(-r\varepsilon))^{0.5} \quad (7)$$

The differentiation of which gives:

$$\frac{d\sigma}{d\varepsilon} = 0.5\sigma_{rec}^2 r\ \exp(-r\varepsilon)(1 - \exp(-r\varepsilon))^{-0.5} \quad (8)$$

Substituting $1 - (\sigma/\sigma_{rec})^2$ for $\exp(-r\varepsilon)$, Eq. (8) can be written as:

$$\frac{d\sigma}{d\varepsilon} = 0.5r\left(\frac{\sigma_{rec}^2 - \sigma^2}{\sigma}\right) \quad (9)$$

The plots of $\sigma\theta = (d\sigma/d\varepsilon)$ versus σ^2 shown in Fig. 1(a) were therefore linearly fitted according to Eq. (9) from which the slope and the

intercept are tantamount to $-0.5r$ and $0.5r\sigma_{rec}^2$, respectively. In the literature, the plot of θ versus σ has been also used for the determination of σ_c, which is the critical stress required for the initiation of DRX [16]. According to the method developed by Poliak and Jonas [23–26], the onset of DRX can be identified as the inflection point of the θ–σ curve near the saturated or peak stress. The observed inflection in the θ–σ curves is associated with the softening due to the first bulges at the early stages of DRX. Fig. 1(b) exhibits the typical plots of θ versus σ used to estimate the critical point from which DRX is started.

Fig. 2indicates the variation of r and σ_{rec} with the Z parameter defined in Eq. (1). The dependence of r and σ_{rec} on Z reflects that the efficiency of DRV decreases as strain rate increases or temperature declines. Substituting the obtained values of r and σ_{rec} in Eq. (7), gives a way to predict the work hardening part of flow curve as shown in Fig. 3. The modeling curves show an acceptable prediction of the experimental flow curves especially at low stress level where DRV is dominant. However, at high stress levels approaching the peak point of flow curve, the modeling and empirical curves deviate due to DRX.

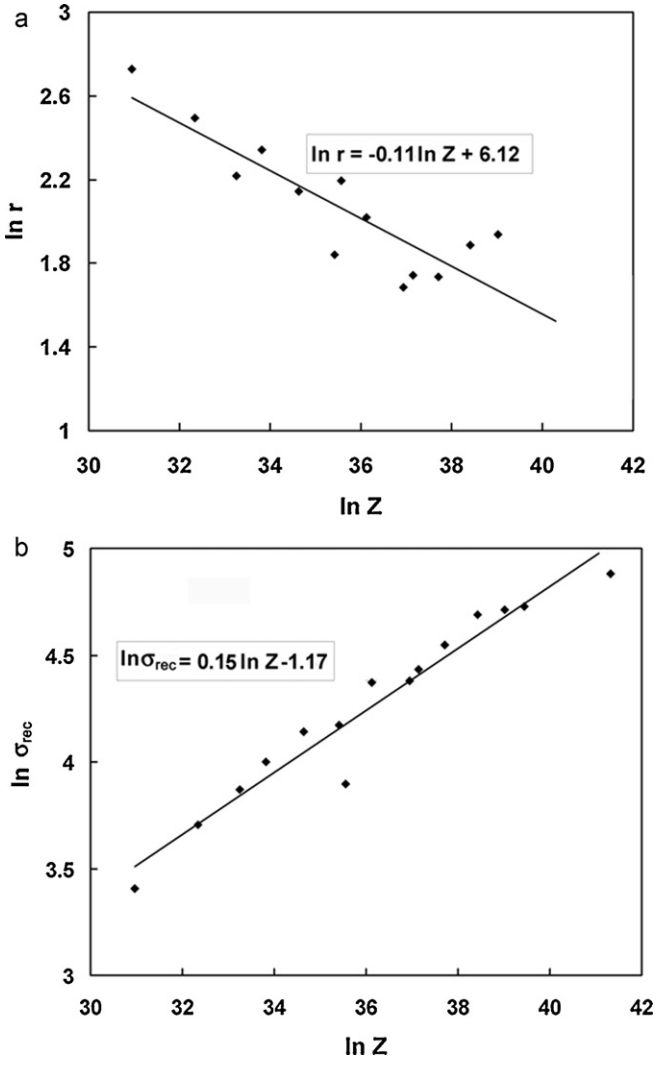

Fig. 2. Variation of (a) dynamic recovery coefficient, r, and (b) the saturation stress of DRV, σ_{rec} with the Zener–Hollomon parameter.

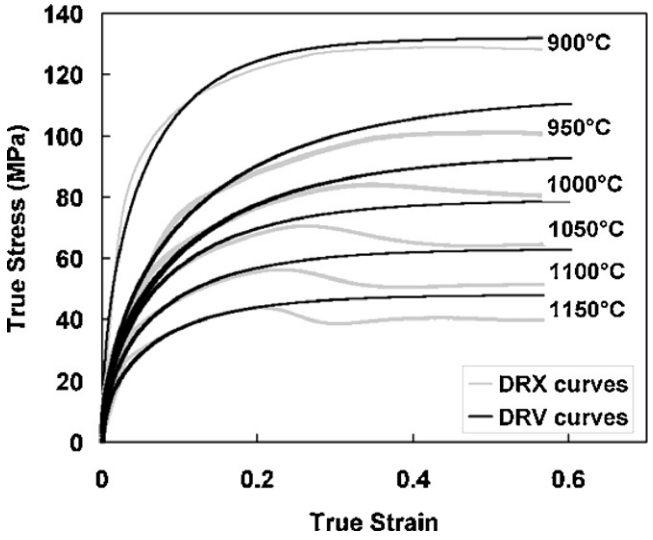

Fig. 3. DRV curves according to Estrin and Mecking's equation used to predict the flow curve of DRX up to the peak.

3.3. Correlation between DRV and DRX

The value of athermal work hardening rate, h, can be calculated from σ_{rec} and r at any deformation condition using the following equation:

$$h = r\left(\frac{\sigma_{rec}}{\alpha MGb}\right)^2 \tag{10}$$

To calculate h, αMGb should be estimated at different deformation conditions. As mentioned earlier α and M can be taken respectively as 1 and 3.07 and G is estimated from simple linear relations with temperature, reported in the literature [17,27]. The shear modulus of different steels in the austenite phase has been proposed as follows [28]:

$$G = 81,000\left[1 - \frac{(T-300)}{1989}\right] \quad (\text{MPa}) \tag{11}$$

where T is the absolute temperature. The magnitude of Burger's vector in austenite is determined from the lattice parameter as $a_0/\sqrt{2}$. a_0 actually depends on the chemical composition as follows [29]:

$$a_0 = 3.573 + 0.033\text{C} + 0.0095\text{Mn} - 0.0002\text{Ni} + 0.0006\text{Cr} + 0.0031\text{Mo} + 0.0018\text{V} \tag{12}$$

Substituting the chemical composition of the studied material mentioned in Table 1, a_0 is obtained about 3.58 Å and therefore, b takes the value of 2.53 Å which is in a good agreement with the values reported in the literature [28,30]. Referring to Eq. (10), the values of h are used to estimate the dislocation density in the steady state regime of DRV. The steady state condition is obviously attained when DRV balances the work hardening and therefore $\theta = d\sigma/d\varepsilon$ is zero. As $\sigma = \alpha MGb\rho^{0.5}$, the steady state regime can be defined as $d\rho/d\varepsilon = 0$. From the evolution law described by Eq. (5), at the steady state condition, the average dislocation density depends on h and r as:

$$\rho_{rec} = \frac{h}{r} \tag{13}$$

Fig. 4 indicates the variation of steady-state dislocation density, ρ_{rec}, with the Z parameter. As observed, ρ_{rec} increases with increasing Z. This is because h increases and r decreases as Z rises. It is worth noting that in case of low and medium SFE materials such as the studied material, DRX starts before the dislocation density reaches

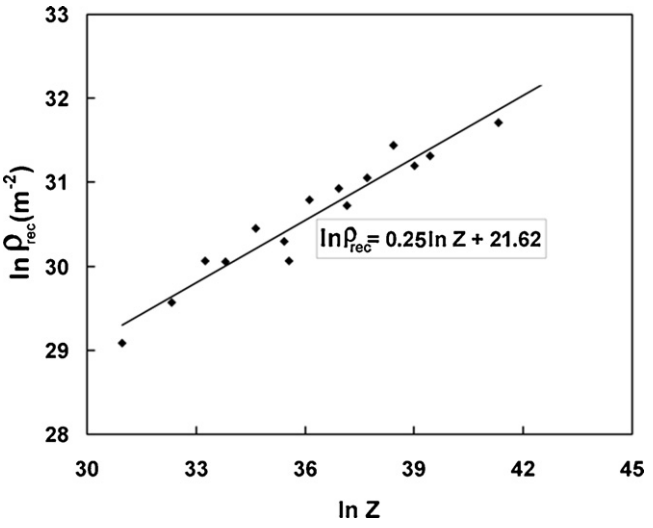

Fig. 4. Variation of the steady state dislocation density, ρ_{rec}, obtained from the DRV model with the Zener–Hollomon parameter.

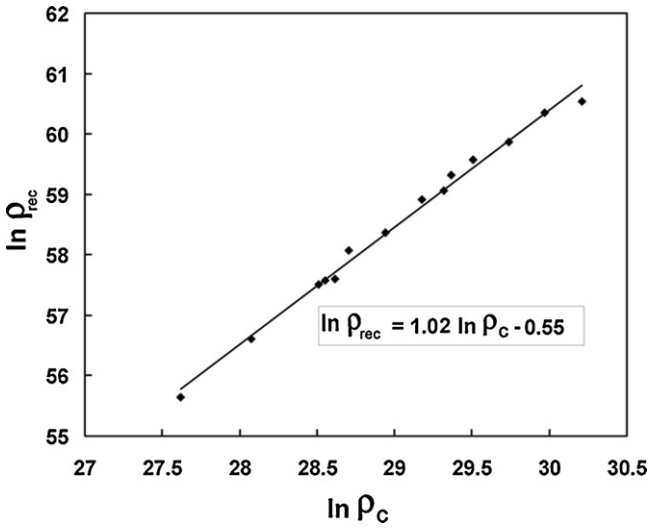

Fig. 6. Dependence of the critical dislocation density for the initiation of DRX, ρ_c, on the steady state dislocation density, ρ_{rec}, obtained from the DRV model.

ρ_{rec}. In order to examine the required condition for the initiation of DRX, the critical strain, ε_c and stress, σ_c, were determined by the method shown in Fig. 1(b). The dependence of ε_c and σ_c on Z is depicted in Fig. 5. Referring to Eq. (3), the ratio of $\varepsilon_c/\varepsilon_p$ takes the average value of 0.8 which is consistent with other reports [31]. The critical strain can be therefore correlated with the corresponding critical dislocation density for starting DRX. For this purpose, the proposed model for the evolution of dislocation density during DRV, Eq. (5), was utilized to calculate the critical dislocation density for the initiation of DRX. Integrating Eq. (5) and substituting ε_c for ε, the critical dislocation density for the initiation of DRX, ρ_c, can be derived as follows:

$$\rho_c = \left(\frac{h}{r}(1 - \exp(-r\varepsilon_c))\right) \tag{14}$$

The plot of ρ_c obtained from Eq. (14) versus ρ_{rec} depicted in Fig. 6 indicates that ρ_c/ρ_{rec} takes the average value of 0.8.

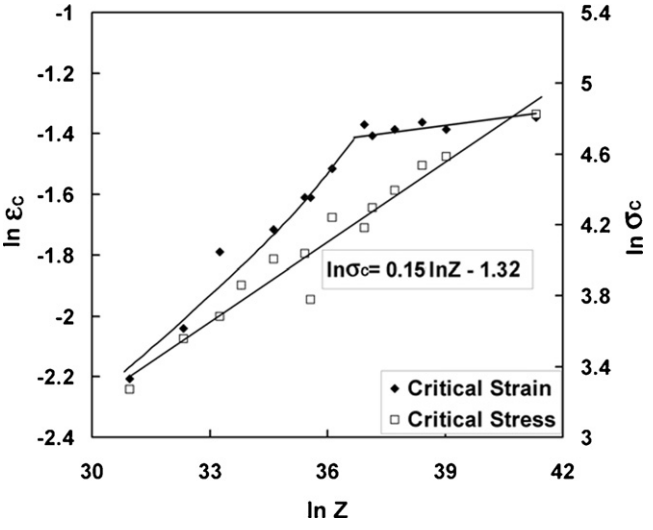

Fig. 5. Dependence of critical strain and stress for the initiation of DRX on with the Zener–Hollomon parameter.

3.4. Verification of critical dislocation density, ρ_c

The critical dislocation density for the initiation of DRX evidently depends on the deformation condition. From the plot shown in Fig. 4, the steady state dislocation density, ρ_{rec}, when DRV is dominant, depends strongly upon the Z parameter. Therefore, from Fig. 6, the dependence of ρ_c to deformation regime can be inferred. However, the dependence of ρ_c to deformation conditions becomes more complicated when DRX also contributes. To clarify this, the variation of ρ_c with the strain rate and the reciprocal of temperature are plotted in Fig. 7. The results indicate that ρ_c bears a modified Arrhenius-type equation with the strain rate and deformation temperature as follows:

$$\rho_c = A\dot{\varepsilon}^p \exp\left(\frac{Q_c}{RT}\right) \tag{15}$$

where A and p are the material constants and Q_c is the activation energy for the initiation of DRX. According to the experimental results, Eq. (15) gives a good description of the critical dislocation density if A, p and Q take the values of 8.2×10^9, 0.3 and 99 kJ mol^{-1}, respectively. In order to formalize the proposed model, the results can be verified by the DRX nucleation criterion proposed by Roberts and Ahlblom [30]. This approach involves the local bulging of a pre-existing high-angle grain boundary into a grain with a critical value of dislocation density which is expressed as:

$$\rho_{crit} = \left(\frac{20S\dot{\varepsilon}}{3blM\tau^2}\right)^{1/3} \tag{16}$$

where S is the grain boundary energy per unit area, b is the magnitude of burger's vector, l denotes the dislocation mean free path, M is the grain boundary mobility and τ is the dislocation line energy. The dislocation mean-free path is approximately equal to the size of subgrains developed during deformation. The sub-grain size depends on the applied stress as follows [32]:

$$l \approx D \approx \frac{10Gb}{\sigma} \tag{17}$$

The mobility of boundary depends actually on the grain boundary diffusion and can be expressed as follows [33]:

$$M = M_0 \exp\left(\frac{-Q_b}{RT}\right) \tag{18}$$

where M_0 is a constant and Q_b denotes the activation energy for the boundary migration. The values of M_0 and Q_b for 18-9 austenitic

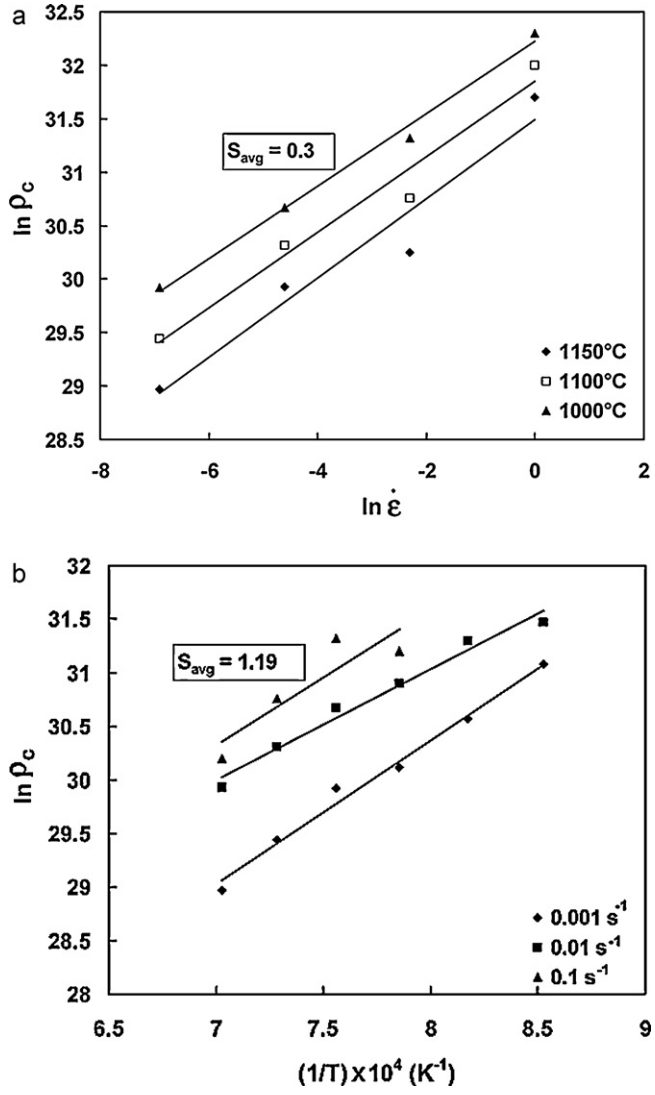

Fig. 7. Dependence of the critical dislocation density for the initiation of DRX, ρ_c, on (a) strain rate and (b) the reciprocal of deformation temperature.

stainless steels have been reported to be $4.1 \times 10^5\ m^4\ J^{-2}\ s^{-1}$ and 420 kJ mol^{-1}, respectively [33]. The dislocation line energy, τ, can be expressed in terms of the magnitude of the Burger's vector and shear modulus as:

$$\tau = \alpha G b^2 \tag{19}$$

Substituting Eqs. (17)–(19) for Eq. (16), the critical dislocation density can be expressed as:

$$\rho_{crit} = \left(\frac{2S\sigma\dot{\varepsilon}}{3\alpha^2 G^3 b^6 M_0 \exp(-Q_b/RT)} \right)^{1/3} \tag{20}$$

Considering $\sigma = \sigma_c = kZ^q$, Eq. (20) can be written as:

$$\rho_{crit} = \left(\frac{2S\dot{\varepsilon} \cdot \{k[\dot{\varepsilon}\exp(Q/RT)]^q\}}{3\alpha^2 G^3 b^6 M_0 \exp(-Q_b/RT)} \right)^{1/3} \tag{21}$$

After doing some algebraic operations, Eq. (21) is therefore finalized as follows:

$$\rho_{crit} = \left(\frac{2kS}{3\alpha^2 G^3 b^6 M_0} \right)^{1/3} \dot{\varepsilon}^{((1+q)/3)} \exp\left(\frac{Q_c}{RT} \right) \tag{22}$$

Referring to Eqs. (15) and (22), the first term on the right-hand side of Eq. (22) is tantamount to A and $p = (1+q)/3$. Considering $\sigma_c = 0.26Z^{0.15}$, from Fig. 5, the value of p is calculated as 0.38 which is in a good agreement with the experimental value of 0.3 obtained from Fig. 7(a). Assuming $Q_b = 420$ kJ mol^{-1}, as mentioned in the literature for austenitic stainless steels [30] and $Q = 440$ kJ mol^{-1} as calculated in the present research, Q_c takes the value of 162 kJ mol^{-1} which is higher than 99 kJ mol^{-1} obtained from the experimental results in Fig. 7(b). One reason for this inconsistency could be the difference in the chemical composition of the low alloy stainless steel used in the present research with that of 18-9 austenitic stainless steels for which Q_b has been reported about 420 kJ mol^{-1} in the literature. The activation energy for boundary migration strongly depends on the grain boundary diffusion of segregated alloying elements. Therefore, the lower alloy content in the studied stainless steel may give rise to lower Q_b that in turn leads to lower Q_c. Considering $S = 0.835$ J m^{-1} and $\alpha = 1$, the critical dislocation density is estimated using Eq. (22) comparing to the results obtained from the experimental model proposed in Eq. (15). The results indicate that the ratio of ρ_{crit}/ρ_c is about 0.3. Considering the values of Q_c obtained from two models and the differences between ρ_c and ρ_{crit}, it seems that the model proposed by Roberts and Ahlblom [30] underestimates the critical dislocation density for the initiation of DRX whereas the proposed model may somewhat overestimate it. This is because in the model proposed by Roberts and Ahlblom [30] the influence of DRV has been neglected; while in the model presented here ρ_c has been predicted utilizing a DRV model which may give rise to some overestimation.

3.5. Evolution of dislocation density during DRX

Based on the theory of strain induced grain boundary migration shown in Fig. 8, the moving bulge sweeps away dislocations while advancing through the deformed matrix [34]. The evolution of dislocation density during DRX can be therefore considered using this model. As observed in Fig. 8, the critical dislocation density in front of the bulge, ρ_c, is decreased to zero and then regenerated by the concurrent deformation behind the moving boundary. Rationally, the dislocation density behind the moving boundary is considered to be a function of position and the amount of deformation after the critical point. In the simplest way, $\rho(x, \varepsilon)$ can be described by:

$$\rho(x, \varepsilon) = \rho'(x) \cdot \rho''(\varepsilon) \tag{23}$$

where $\rho'(x)$ and $\rho''(\varepsilon)$ express the dependence of regenerated dislocation density to position and strain after the critical point, respectively. The evolution of dislocation density behind the DRX bulge obeys the generation and annihilation mechanisms during DRV. Therefore, the evolution function described by Eq. (5) can be used to explain the variation of regenerated dislocation density with strain as follows:

$$\rho''(\varepsilon) = \frac{h}{r}[1 - \exp(-r\varepsilon)] \tag{24}$$

Roberts and Ahlblom [30] showed that the dislocation density regenerated bears a linear dependence upon the position behind the moving bulge as:

$$\rho(x) = \frac{\dot{\varepsilon}}{blM\tau\rho_c} \cdot x \tag{25}$$

According to Eq. (17), the dislocation mean-free path is approximated to $10Gb/\sigma$. Considering $\sigma = \alpha Gb\sqrt{\rho}$, the dislocations mean-free path is related to the dislocation density as follows:

$$l \approx D = \frac{10}{\sqrt{\rho}} \tag{26}$$

This expression can be combined with Eqs. (23)–(25) as follows:

$$\rho(x, \varepsilon)\big|_{DRX} = \frac{\dot{\varepsilon}x}{10bM\tau\rho_c} \cdot \left\{ \frac{h}{r}[1 - \exp(-r(\varepsilon - \varepsilon_c))] \right\}^{1/2} \tag{27}$$

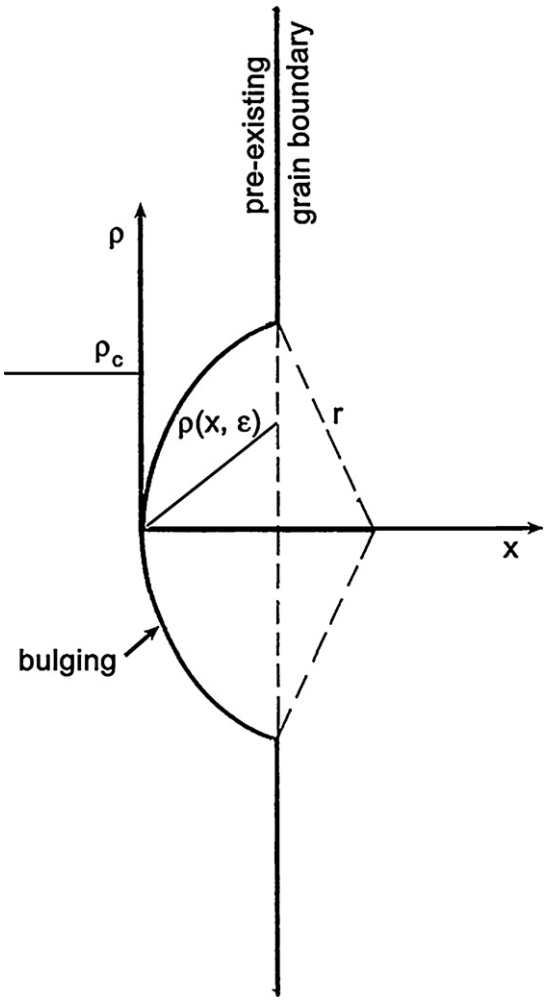

Fig. 8. Schematic illustration of the SIBM mechanism of DRX nucleation with the corresponding change in the dislocation density.

According to Eq. (27), at a given position, dislocations are regenerated behind the moving boundary so that the dislocation density reaches a maximum at the peak point of flow curve. Nearly at the peak the pre-existing grain boundaries are totally occupied by a layer of DRX grains which is termed as "necklace structure". The average dislocation density at the peak can be therefore written as follows:

$$\bar{\rho}(\varepsilon_p)\big|_{\mathrm{DRX}} = \frac{1}{r'}\int_0^{r'} \rho(x,\varepsilon_p)dx \tag{28}$$

Here r' denotes the radius of grains which can be considered identical to the critical radius of DRX nuclei. Integrating from Eq. (28) yields:

$$\bar{\rho}(\varepsilon_p)\big|_{\mathrm{DRX}} = \frac{\dot{\varepsilon}r'}{20bM\tau\rho_c}\cdot\left\{\frac{h}{r}[1-\exp(-r(\varepsilon_p-\varepsilon_c))]\right\}^{1/2} \tag{29}$$

The value of r' can be obtained from the analysis of Roberts and Ahlblom [30] as follows:

$$r' = \frac{3bDM\tau}{5\dot{\varepsilon}}\cdot\rho_c^2 \tag{30}$$

Assuming $D \approx 10/\sqrt{\rho_p}$ at the peak point, Eq. (30) can be combined with Eq. (29) to form a simple following relation as follows:

$$\bar{\rho}(\varepsilon_p)\big|_{\mathrm{DRX}} = \frac{3}{10}\rho_c \tag{31}$$

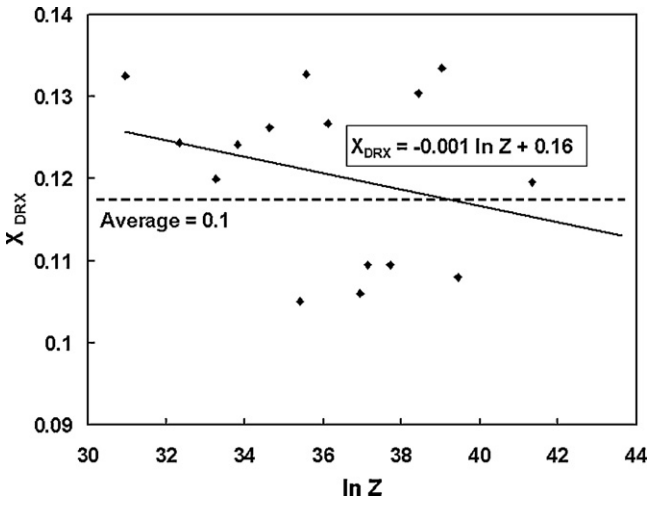

Fig. 9. Predicted fractional softening due to DRX at the peak point of flow curve versus the Z parameter. X_{DRX} reaches the average value of 0.1 at the peak and remains nearly constant at different deformation regimes.

Albeit, it is evident that $\bar{\rho}(\varepsilon_p)\big|_{\mathrm{DRX}}$ is pertaining to a part of microstructure in which DRX has taken place and other parts have just undergone DRV. The total density of dislocation in the structure at the peak can be therefore expressed as follows:

$$\bar{\rho}_{tot}(\varepsilon_p) = X_{\mathrm{DRX}}\bar{\rho}(\varepsilon_p)\big|_{\mathrm{DRX}} + (1-X_{\mathrm{DRX}})\,\bar{\rho}(\varepsilon_p)\big|_{\mathrm{DRV}} \tag{32}$$

where X_{DRX} denotes the fractional softening at the peak due to DRX and $\bar{\rho}(\varepsilon_p)\big|_{\mathrm{DRV}}$ is determined from Eq. (24) for $\varepsilon = \varepsilon_p$. Combining Eqs. (31) and (32) with the expression of $\bar{\rho}_{tot}(\varepsilon_p) = \sigma_p^2/(\alpha MGb)^2$, the fractional softening of DRX at the peak is given by:

$$X_{\mathrm{DRX}}\big|_{\varepsilon=\varepsilon_p} = \frac{(\sigma_p^2/(\alpha MGb)^2) - \bar{\rho}(\varepsilon_p)\big|_{\mathrm{DRV}}}{\bar{\rho}(\varepsilon_p)\big|_{\mathrm{DRX}} - \bar{\rho}(\varepsilon_p)\big|_{\mathrm{DRV}}} \tag{33}$$

It was mentioned earlier that all the terms on the right-hand side of Eq. (33) are functions of Z and therefore X_{DRX} at the peak should depend on deformation condition. But, as observed in Fig. 9, X_{DRX} at the peak point of flow curve decreases gently with increasing Z so that it can be considered nearly independent of Z. The values of X_{DRX} were calculated in range of 0.06–0.15 and the average value obtained about 0.1 which is in a good agreement with previous reports [16].

It is evident that during DRX dislocation regeneration is controlled not only by DRV but also by the speed and mobility of the moving boundary. Hence, to estimate the dislocation density during DRX, it is necessary to present an evolution function describing the velocity of the moving bulge. The velocity of a moving boundary depends on its radius, mobility and driving pressure as follows:

$$V = \frac{r'}{t} = MP \tag{34}$$

Here r' is the instant radius of bulging, t is time after the initiation of DRX and M and P denote the boundary mobility and moving pressure, respectively. The net pressure propelling a bulge during the early stages of DRX arises from the difference of dislocation density on the sides of the moving boundary. As the dislocation density decreases from ρ_0 to zero, according to Fig. 8, the driving pressure for bulging is defined as follows:

$$P = \tau\rho_c \tag{35}$$

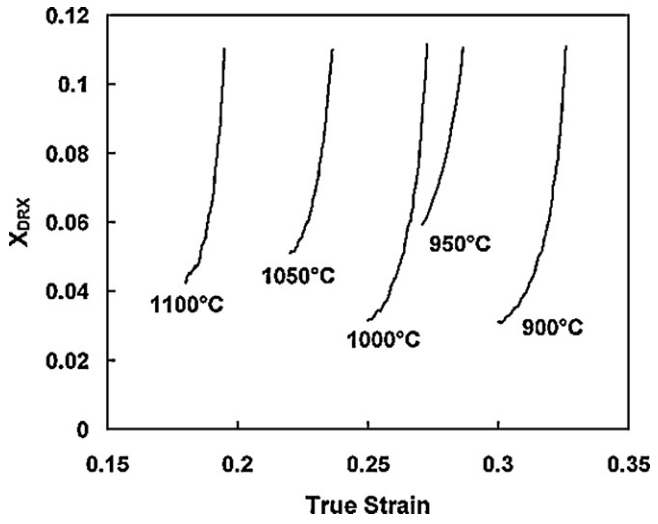

Fig. 10. Variation of DRX fractional softening with strain from ε_c to ε_p. The experimental data comprise a part of the sigmoidal curve of X_{DRX} with strain according to the Avrami's kinetics equation.

The time taken to a bulge reach a given radius can be defined as the ratio of instant strain to the applied strain rate. Therefore, Eq. (34) can be rewritten to the following form:

$$r' = \frac{M\tau\rho_c(\varepsilon - \varepsilon_c)}{\dot{\varepsilon}} \tag{36}$$

Substituting r' in Eq. (36) for x in Eq. (28) and considering instant ε instead of ε_p gives a new model for the estimation of the average dislocation density after the initiation of DRX:

$$\bar{\rho}(\varepsilon)\big|_{DRX} = \frac{\varepsilon - \varepsilon_c}{20b} \cdot \left\{ \frac{h}{r}[1 - \exp(-r(\varepsilon - \varepsilon_c))] \right\}^{1/2} \tag{37}$$

Using Eqs. (24), (33) and (37), the fractional softening due to DRX can be generalized for any given strain from ε_c to ε_p as follows:

$$X_{DRX} = \frac{(\sigma/(\alpha MGb))^2 - (h/r)[1 - \exp(-r\varepsilon)]}{((\varepsilon - \varepsilon_c)/20b)\{(h/r)[1 - \exp(-r(\varepsilon - \varepsilon_c))]\}^{1/2} - (h/r)[1 - \exp(-r\varepsilon)]} \tag{38}$$

Fig. 10 exhibits the results of Eq. (38) versus true strain at different deformation temperatures and constant strain rate of 0.01 s^{-1}. It is obviously seen that the results consist a part of the sigmoidal curve of X_{DRX} with strain which is also expected from the Avrami's kinetics equation.

4. Conclusions

The dynamic recrystallization and flow curve of 410 martensitic stainless steel was analyzed and modeled by means of a dynamic recovery model. The major conclusions are listed below:

1. The Estrin and Mecking's equation for dynamic recovery was used to model the work hardening part of the flow curve.
2. The critical strain and stress for the initiation of DRX were determined using the method proposed by Poliak and Jonas. The critical dislocation density for starting DRX was estimated using the DRV model.
3. A modified Arrhenius-type equation was used to relate the critical dislocation density to strain rate and temperature.
4. The presented model for the estimation of critical dislocation density was verified by the model proposed by Roberts and Ahlblom. It was found that Roberts and Ahlblom's model bears some underestimation, whereas our results may exhibit some overestimation.
5. The DRV model was utilized to understanding the dislocation density evolution during DRX. The fractional softening of DRX at the peak point of flow curve was found about 10% and nearly independent of Z parameter. The variation of X_{DRX} with strain up to the peak in flow curve was observed to be sigmoidal and consistent with the Avrami's kinetics equation.

References

[1] A.S. Taylor, P.D. Hodgson, Mater. Sci. Eng. A528 (2011) 3310–3320.
[2] A. Momeni, A. Shokuhfar, S.M. Abbasi, J. Mater. Sci. Technol. 23 (2007) 775–778.
[3] S. Kim, Y.C. Yoo, Mater. Sci. Eng. 311 (2001) 108–113.
[4] M. El Wahabi, L. Gavard, F. Montheillet, J.M. Cabrera, J.M. Prado, Acta Mater. 53 (2005) 4605–4612.
[5] S.I. Kim, Y.C. Yoo, Mater. Sci. Eng. A311 (2001) 108–113.
[6] A. Momeni, K. Dehghani, H. Keshmiri, G.R. Ebrahimi, Mater. Sci. Eng. A527 (2010) 1605–1611.
[7] T. Maki, K. Akasaka, K. Okuno, I. Tamura, Trans. ISIJ 22 (1982) 253–261.
[8] S. Venugopal, S.L. Mannan, P. Rodriguez, J. Mater. Sci. 39 (2004) 5557–5560.
[9] N.D. Ryan, H.J. McQueen, J. Mater. Proc. Technol. 21 (1990) 177–199.
[10] A. Dehghan-Manshadi, P.D. Hodgson, J. Mater. Sci. 43 (2008) 6272–6277.
[11] S. Venugopal, S.L. Mannan, Y.V.R.K. Prasad, Met. Trans. A 23 (1992) 3093–3103.
[12] L. Gavard, F. Montheillet, J. Le Coze, Mater. Trans. JIM 41 (2000) 113–115.
[13] A. Momeni, K. Dehghani, G.R. Ebrahimi, H. Keshmiri, Met. Mater. Trans. 41A (2010) 2898–2904.
[14] A. Momeni, K. Dehghani, Met. Mater. Int. 5 (2010) 843–849.
[15] A.M.J. Junior, O. Balancin, Mater. Res. 8 (2005) 309–315.
[16] J.J. Jonas, X. Quelennec, L. Jiang, E. Martin, Acta Mater. 57 (2009) 2748–2756.
[17] E.S. Puchi Cabrera, J. Eng. Mater. Technol. 123 (2001) 301–308.
[18] S. Serajzadeh, J. Eng. Mater. Technol. 126 (2004) 406–412.
[19] A. Yoshie, T. Fujita, M. Fujioka, K. Okamoto, H. Morikawa, ISIJ Int. 36 (1996) 467–473.
[20] Y. Estrin, H. Mecking, Acta Metall. 32 (1984) 57–70.
[21] A. Cingara, H.J. Mcqueen, J. Mater. Process. Technol. 36 (1992) 31–42.
[22] C.M. Sellars, W.J. Mc, G. Tegart, Int. Met. Rev. 17 (1972) 1–10.
[23] J.J. Jonas, E. Poliak, Mater. Sci. Forum 426–432 (2003) 57–66.
[24] E.I. Poliak, J.J. Jonas, Acta Mater. 44 (1996) 127–136.
[25] E.I. Poliak, J.J. Jonas, ISIJ Int. 43 (2003) 684–691.
[26] E.I. Poliak, J.J. Jonas, ISIJ Int. 43 (2003) 692–700.
[27] H.J. Frost, M.F. Ashby, Deformation-Mechanism Maps, The Plasticity and Creep of Metals and Ceramics, Pergamon Press, Cambridge, 1982.
[28] A. Taylor, B.J. Kagle, Crystallographic Data on Metal and Alloy Structures, Dover Publications Inc., 1982.
[29] F.G. Caballero, C. Capdevila, C. Garcia De Andres, J. Mater. Sci. 37 (2002) 3533–3540.
[30] W. Roberts, B. Ahlblom, Acta Metall. 26 (1978) 801–813.
[31] S.I. Kim, Y.C. Yoo, Mater. Sci. Eng. A311 (2001) 108.
[32] D. Kuhlmann-Wilsdorf, J.H. Wan der merwe, Mater. Sci. Eng. 55 (1982) 79–83.
[33] Y. Brechet, Y. Estrin, F. Reusch, Scr. Mater. 39 (1998) 1191–1197.
[34] F.J. Humphreys, M. Hatherly, Recrystallization and Related Annealing Phenomena, second ed., Pergamon, Netherlands, 2004, pp. 251–257.